

## Figures

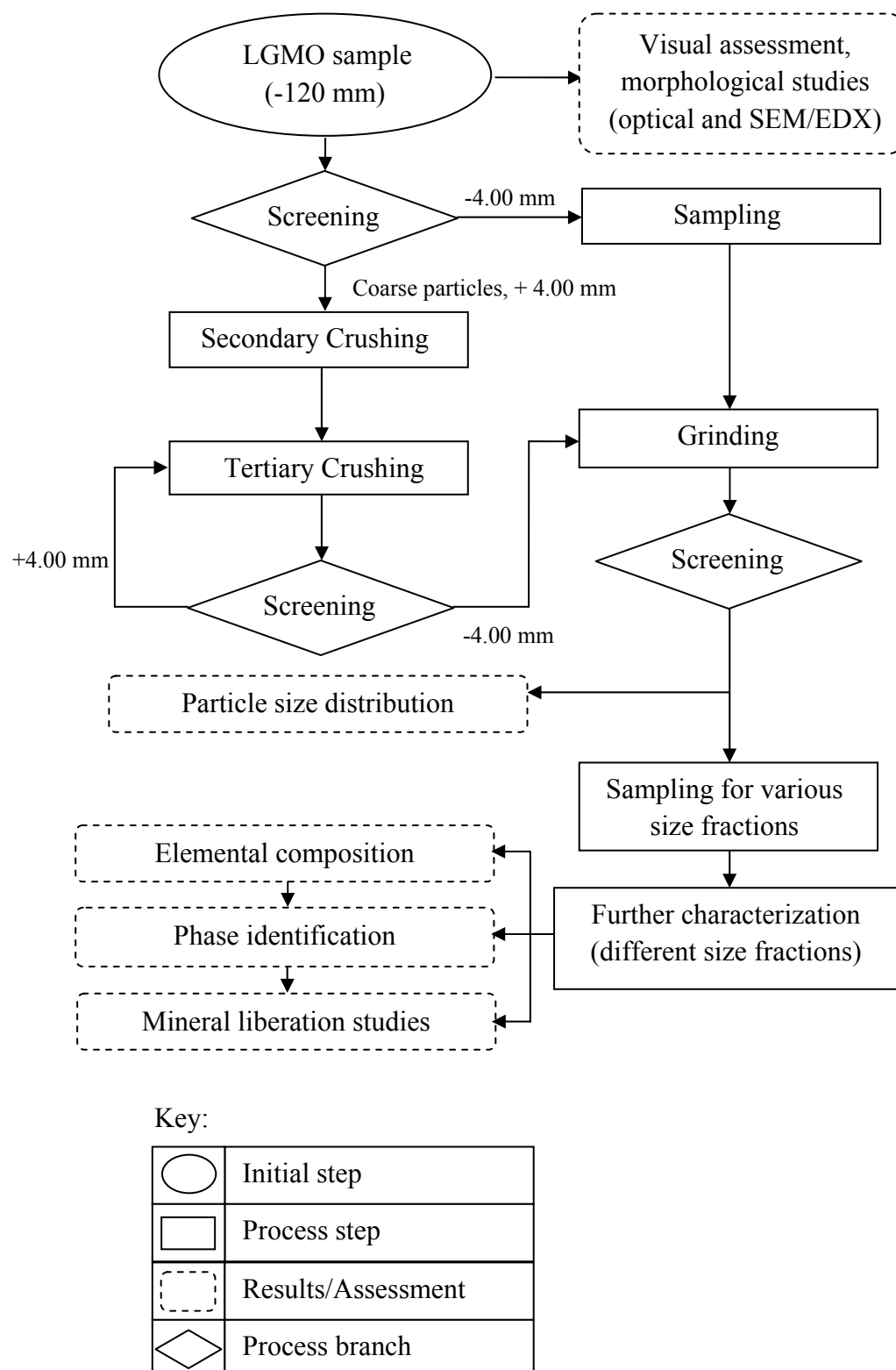


Figure 1: A flowchart depicting the stages involved in the characterization of LGMO in this work.



Figure 2: Visual assessment of Sungai Temau's LGMO, the sample for this work.

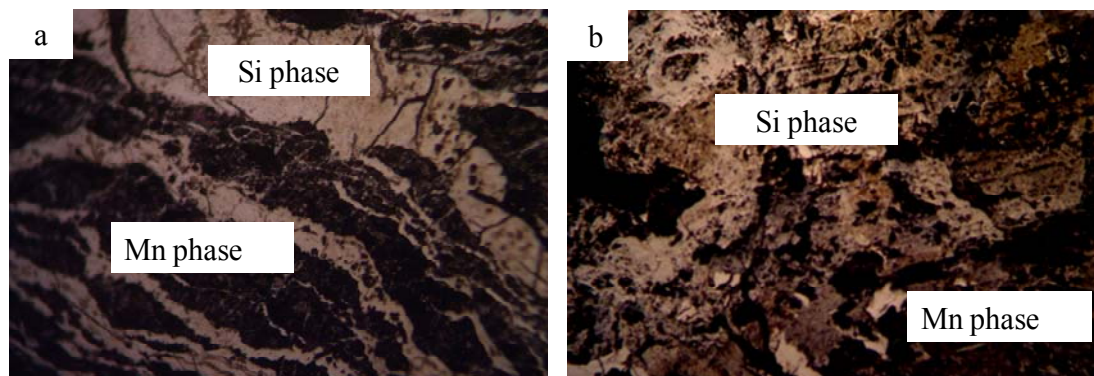


Figure 3: Optical microscope micrograph showing the complexity of mineralogy and texture of LGMO. Total magnification=3958X, (a) Zoning structure of Mn and Si phases, (b) Disseminated Mn phase in Si rich phase. Identification was done by EDX.

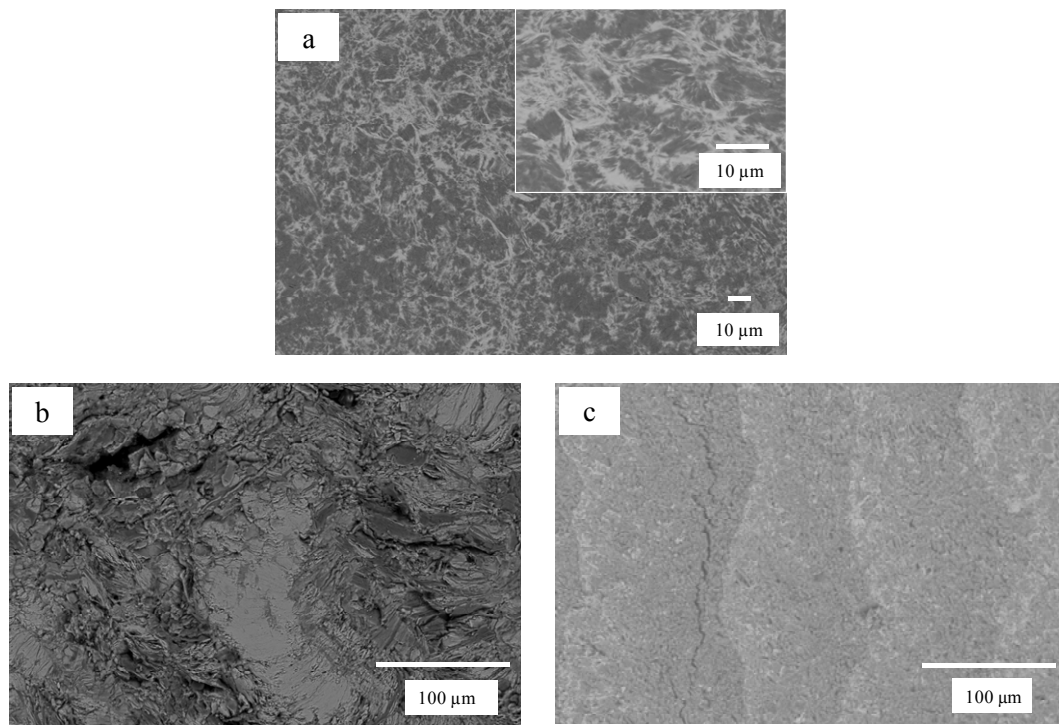


Figure 4: BSI photomicrograph of (a) Very fine manganese and aluminium-iron phase's intergrowth in quartz gangue, (b) fibrous manganese rich phase contained aluminium-iron phases, (c) zoning structure of different grey level of manganese and aluminium-iron phases.

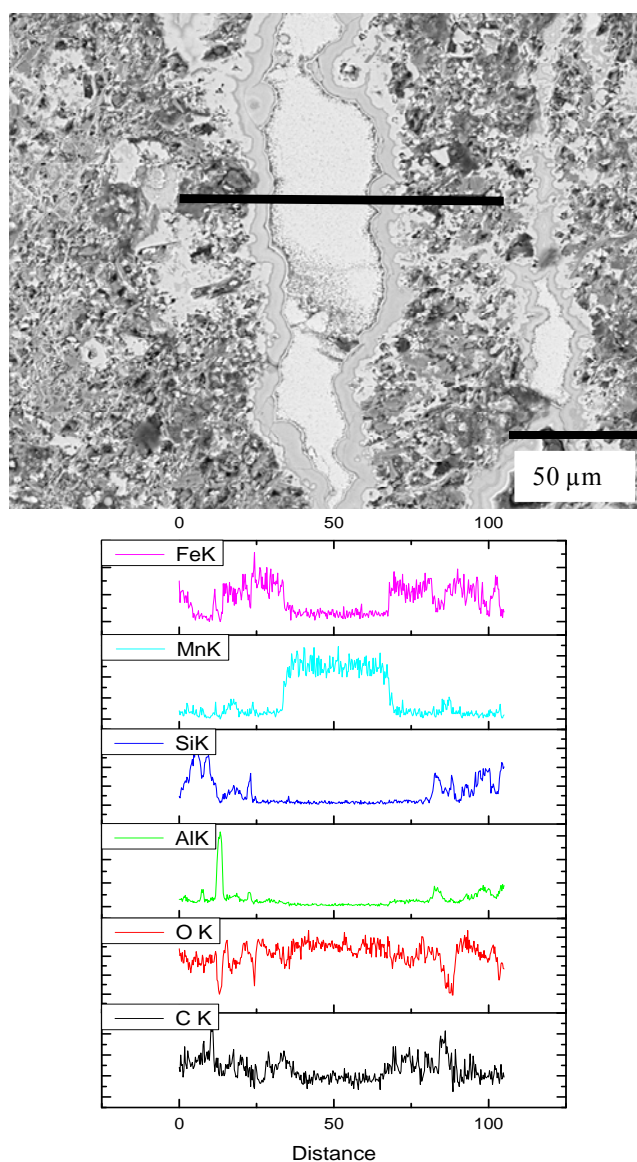


Figure 5: (Top) BSI photomicrograph of the Malaysian LGMO and (bottom) EDX linescan analysis showing compositional variation within the LGMO.

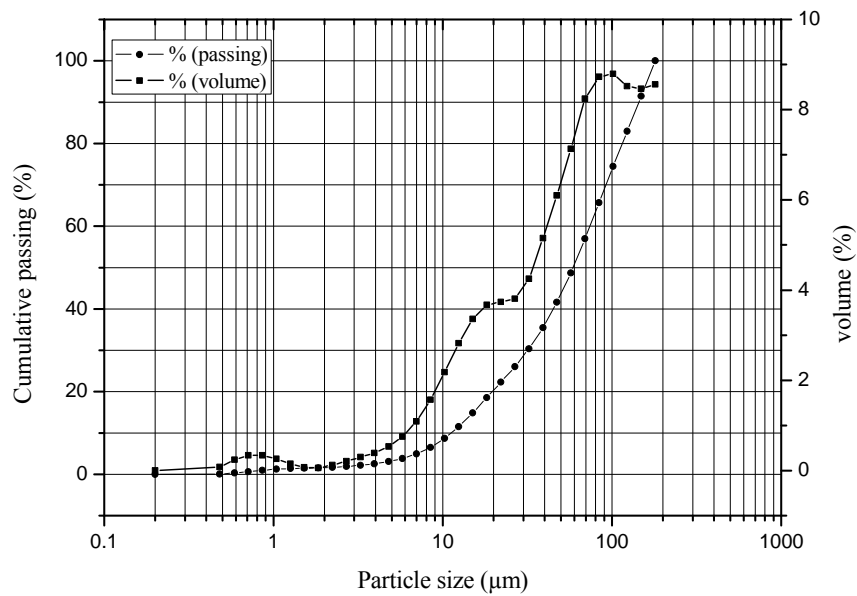


Figure 6: PSD of ground LGMO  $\leq 75\mu\text{m}$ ; cumulative and volume distribution curves.

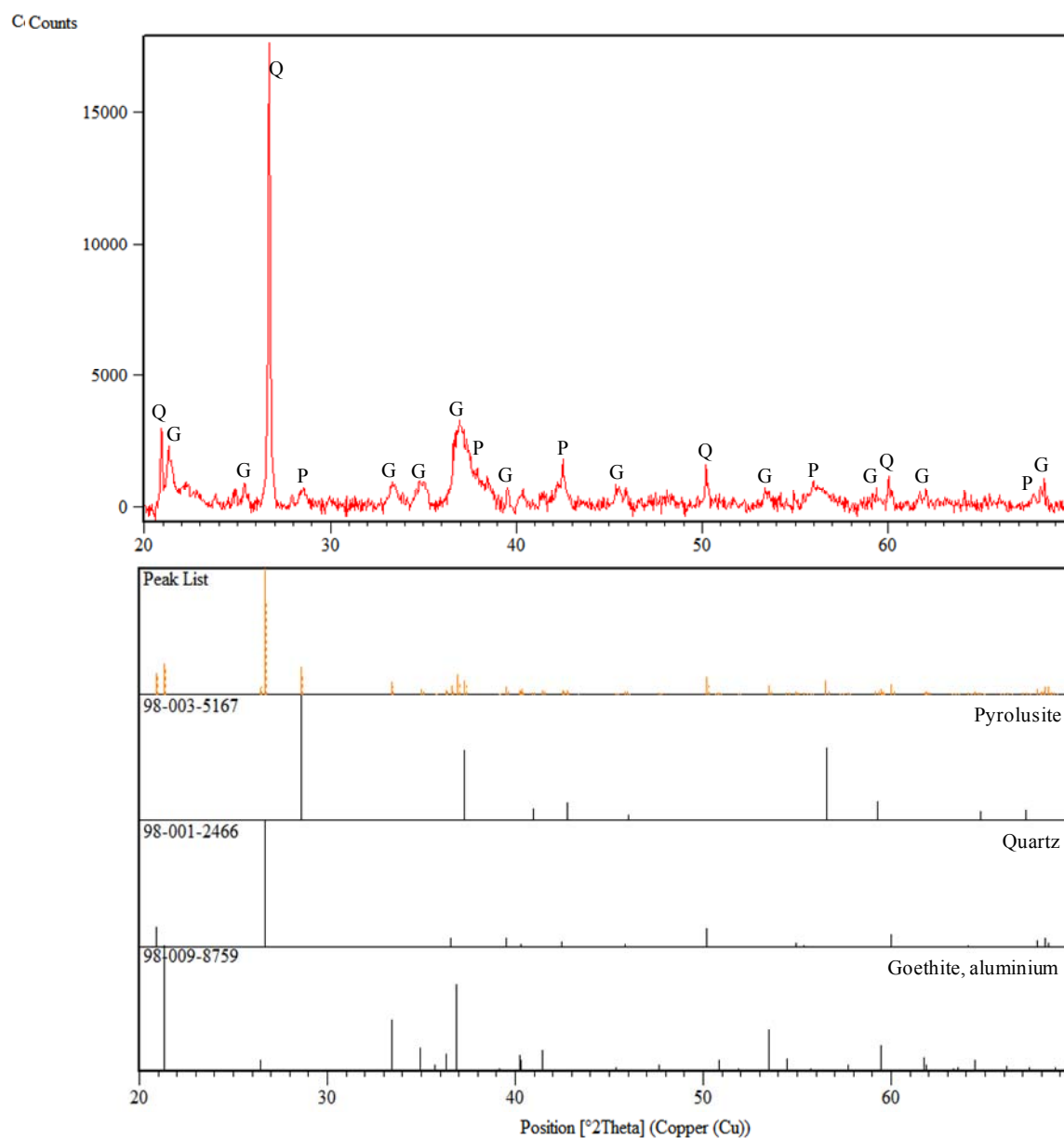


Figure 7: XRD pattern of LGMO samples. Abbreviations: Q, Quartz; P, Pyrolusite; G, Aluminium-substituted goethite.

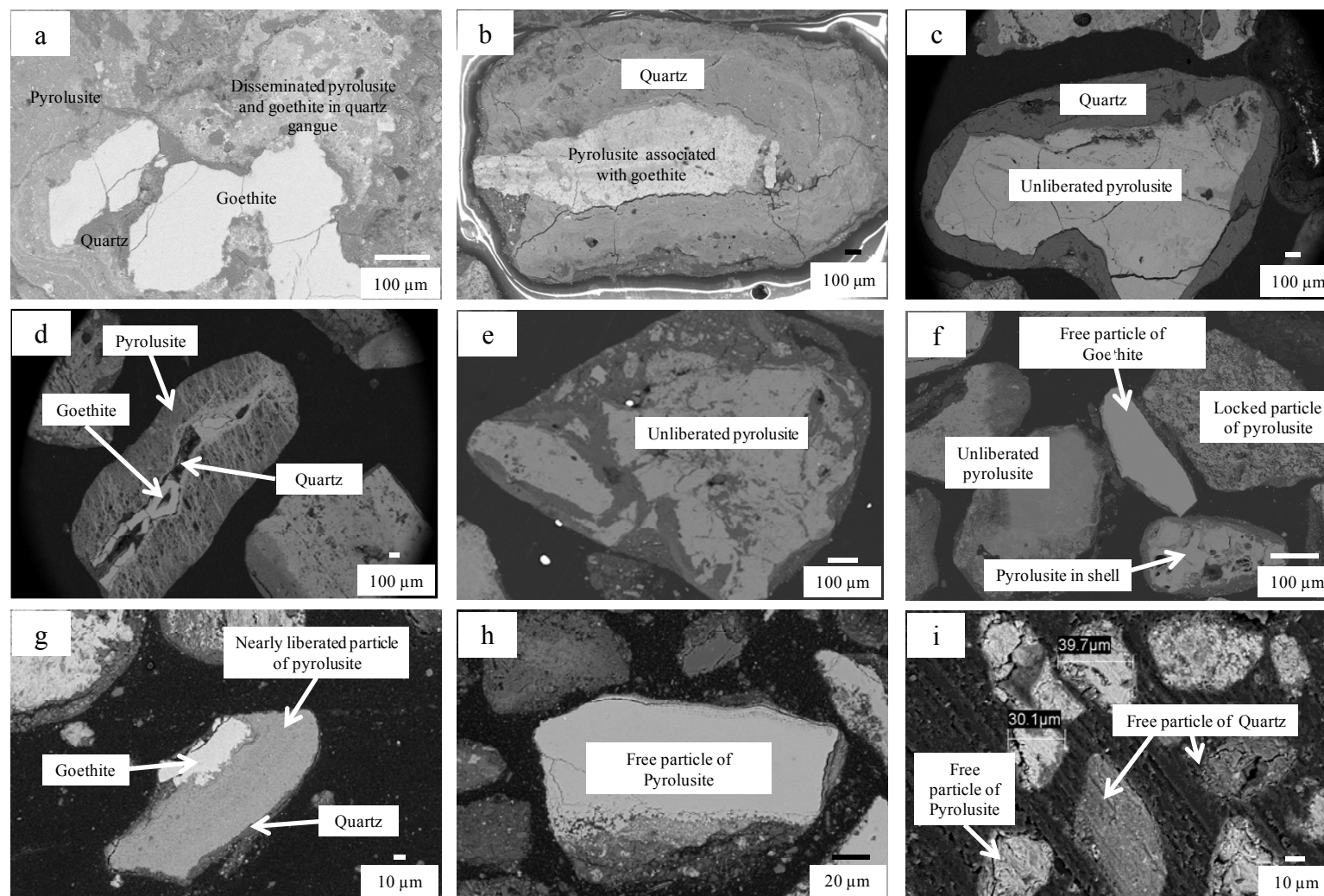


Figure 8: BSI of nine sample micrographs to distinguish the degree of mineral liberation at different LGMO size fractions. (a) Refers to  $(-4.00+3.35)\text{mm}$ , (b)  $(-3.35+2.8)\text{mm}$ , (c)  $(-2.80+1.18)\text{mm}$ , (d)  $(-1180+500)\mu\text{m}$ , (e)  $(-500+350)\mu\text{m}$ , (f)  $(-350+250)\mu\text{m}$ , (g)  $(-250+150)\mu\text{m}$ , (h)  $(-150+75)\mu\text{m}$ , and (i)  $-75\mu\text{m}$ .



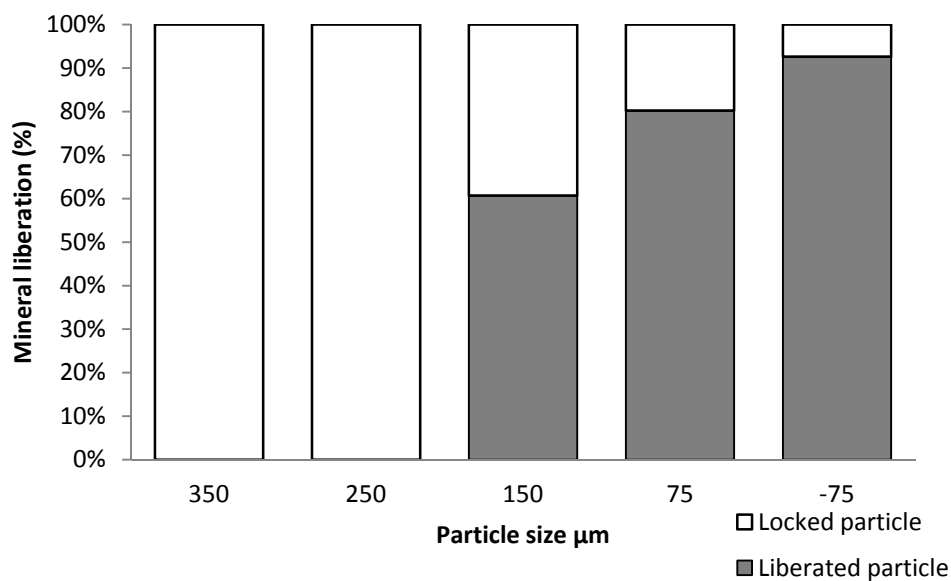


Figure 9: Percentage of liberation obtained from image analysis of particles as per Figure 6 (e-i), i.e., particle size fractions of  $(-350+250)$   $\mu\text{m}$ ,  $(-250+150)$   $\mu\text{m}$ ,  $(-150+75)$   $\mu\text{m}$ , and  $-75$   $\mu\text{m}$ , respectively. Percentage of liberation was calculated as per equation (2) in section 2.6.